Hanwu LUO[1], Peng CHENG[2], Haibo LIU[1], Kai KANG[1], Fan YANG[2], Qi YANG[2]

East Inner Mongolia Electric Power Company Limited (1), Chongqing University (2)

doi:10.15199/48.2016.06.17

Investigation of the Needle-plate Discharge Characteristics in Atmospheric Air Based on Coupling Fields

Abstract. *In order to investigate the partial discharge characteristics, a needle-plate discharge model was proposed, which is built on the base of magneto-hydrodynamic (MHD) theory, is taken as an example. Based on this model, the distributions of coupling fields can be calculated. The simulation results are helpful for us to understand the fundamental characteristics in the process of partial discharge.*

Streszczenie. *W celu zbadania charakterystyk wyładowań niezupełnych zaproponowano model wyładowania igła-płyta zbudowany na bazie teorii magnetohydrodynamicznej (MHD). Na podstawie tego modelu możliwe jest obliczenie rozkładu pól sprzężonych. Wyniki symulacji są użyteczne do zrozumienia podstawowych charakterystyk w procesie wyładowania niezupełnego.* ***(Badanie charakterystyk wyładowania „igła-płyta" w powietrzu z wykorzystaniem pól sprzężonych).***

Keywords: Partial discharge, Needle-plate discharge, Magneto-hydrodynamic (MHD), Coupling fields.
Słowa kluczowe: Wyładowanie niezupełne, Rozładowanie igła-płyta, Magnetohydrodynamika (MHD), Pola sprzężone.

Introduction

Partial discharge (PD), as a potential threat directly affects the insulation, safety of electrical equipment in power systems. Partial discharge process is a complicated phenomenon, which includes a mutual coupling between flow field, electromagnetic field and thermal field. In the state of art, many scholars focus on the arc investigation through experimental methods. Due to the development of computer technology, it is possible for us now a day to investigate this problem by using simulation method [1-3].

In this paper, a needle-plate discharge model is built based on magneto-hydrodynamic (MHD) theory. Through the mathematical calculation, the distributions of the electric, temperature and flow fields are investigated.

Methodology

A. Assumptions

In the study of macroscopic, the movement of the plasma discharge, the air between the two electrodes is usually handled as compressible fluid. The characteristic is that conductive particles are included in this fluid. The physical parameters including density, viscidity coefficient, thermal conductivity and electrical conductivity are the functions of temperature [4]. The needle-plate discharge model is based upon the following assumptions are as follows:

1) First, the discharge plasma satisfies the conditions for local thermodynamic equilibrium.

2) Second, the plasma is a Newtonian fluid, and the flow is laminar [5-6].

3) Third, the arc-electrode interaction has not taken into account.

4) Fourth, the space charge layer near the electrodes has not taken into account.

5) Fifth, the impact of induced current of the total current can be ignored.

B. Governing Equations

Based on the MHD theory, the flow field in the process of needle-plate discharge can be described by the equations of conservation of mass (1), momentum (2) and energy (3) [7-10].

$$\frac{\partial \rho}{\partial t}+\operatorname{div}(\rho \mathbf{v})=0 \tag{1}$$

$$\frac{(\partial \rho v_i)}{\partial t}+\operatorname{div}(\rho \mathbf{v} v_i)=-\frac{\partial p}{\partial x_i}+\operatorname{div}(\eta \operatorname{grad} v_i)+(\mathbf{J}\times\mathbf{B}) \tag{2}$$

$$\frac{(\partial \rho H)}{\partial t}+\operatorname{div}(\rho \mathbf{v} H)-\operatorname{div}(\lambda \operatorname{grad} T)=\frac{\partial p}{\partial t}-S_R+\frac{1}{\sigma}\mathbf{J}^2 \tag{3}$$

Where: t is time, v_i is the component of velocity in rectangular coordinates, P is pressure, T denoted temperature, H represent the enthalpy, $\mathbf{J}$ denote current density, $\mathbf{B}$ is magnetic induction intensity, S_R denoted radiation loss, ρ is density, η is viscosity, λ represent thermal conductivity, σ is the electrical conductivity.

The electric field and current density can be determined by the Maxwell equations.

$$\operatorname{div}(\sigma \operatorname{grad}\varphi)=0 \tag{4}$$

$$\mathbf{J}=-\sigma \operatorname{grad}\varphi \tag{5}$$

where: φ is electric potential.

The magnetic field can be obtained by calculating the magnetic vector potential A_i (i=r, ϕ, z).

$$\nabla\cdot(\nabla A_i)=-\mu_0 J_i \tag{6}$$

where: μ_0 is relative permeability.

And magnetic flux density **B** is calculated from the equation (7).

$$\mathbf{B}=\nabla\times\mathbf{A} \tag{7}$$

Example Simulation and Analysis

A. Geometry model and boundary conditions

The needle-plate discharge model is built in 2-D axial symmetry configurations, as shown in Fig.1. The radius of the curvature at the needle tip is 0.2 mm. The ground electrode is set 1 cm away from the needle electrode. The domain dimensions chosen are 2 cm to 3 cm.

The boundary conditions are as follows:

1) At the needle-electrode, the simulation voltage is set to a sinusoidal voltage. The ground electrode is grounded via a shielded low inductance 1 Ω shunt resistance.

2) At the open boundaries, the static pressure is equal to zero and the temperature is set to the ambient temperature of 293.15 K.

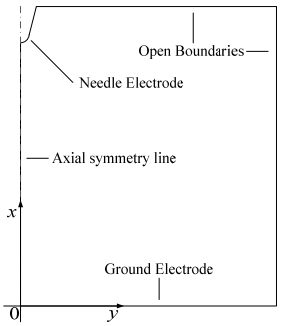

Fig.1. Needle-plate discharge system simulation geometry.

B. Calculation method and mesh generation

The equations in the discharge simulation have strong coupling with each other. A double iterative algorithm is used to calculate this coupling model and the calculation flow chart is shown in Fig.2.

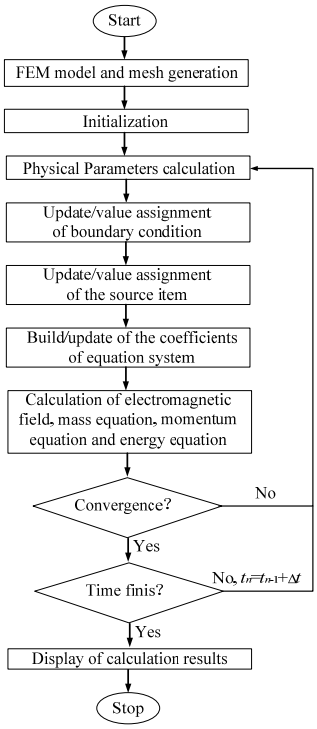

Fig.2. The program diagram of computational process.

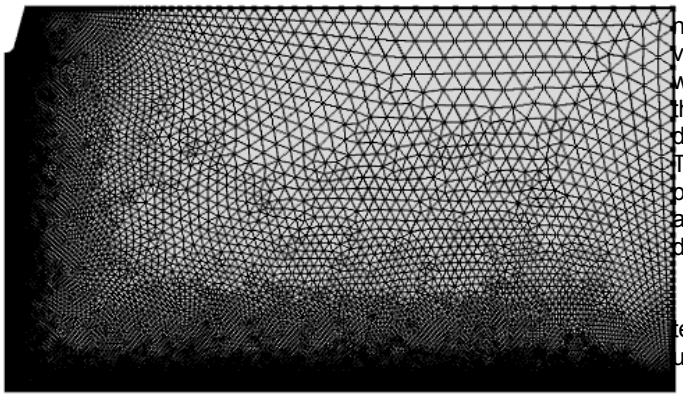

Fig.3. Finite element mesh generation of needle-plate model.

The triangular meshes are used to subdivide the discharge region in finite element software. In order to improve the computing precision and obtain a better convergence, the uneven mesh generation has been adopted. The finite element mesh generation of the needle - plate model is shown in Fig.3.

C. Simulation results and discussions

Fig.4 and Fig.5 show the voltage and current of needle-plate discharge plasma for a voltage of 2000 V during one full cycle.

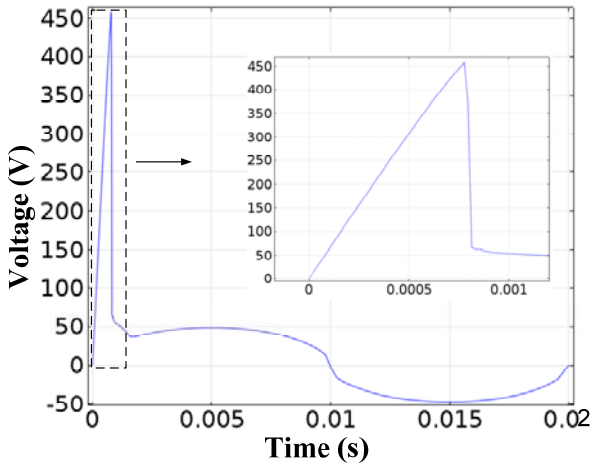

Fig.4. Waveform of the voltage of the needle-plate.

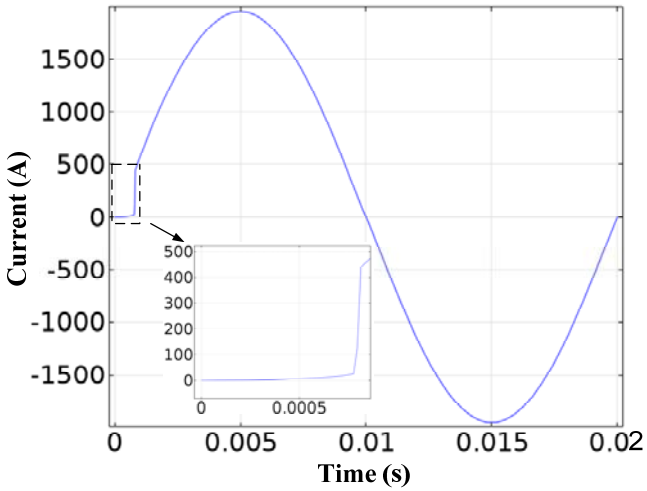

Fig.5. Waveform of the discharge current of the needle-plate.

It can be observed that the breakdown time of the needle-plate gap was t=0.78 ms. Before the breakdown, the voltage and discharge current of the needle-plate increase with time, but the discharge current is almost zero. Once the needle-plate gap is a breakdown, the voltage is instantly decreased and the discharge current is instantly increased. This is because the resistance between the needle and plate can be considered to be infinity before breakdown and a small constant after breakdown. Then the voltage and discharge current changing sinusoidal with the time.

Fig.5-Fig.7 show the electric potential, electric field and temperature distribution of needle-plate discharge plasma under four different times before breakdown.

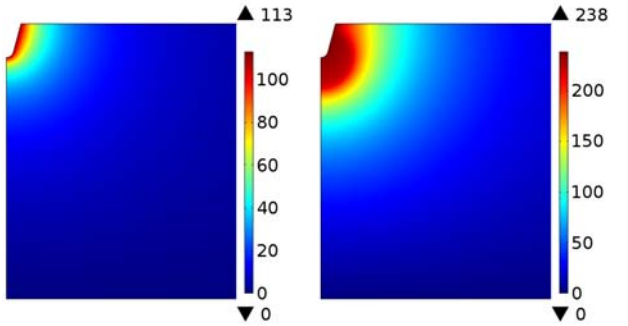

(a) *t*=0.18 ms (b) *t*=0.38 ms

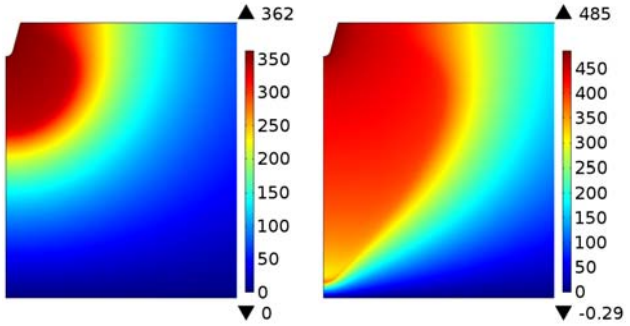

(c) *t*=0.58 ms (d) *t*=0.78 ms

Fig.5. Electric potential distributions before the breakdown of needle-plate gap.

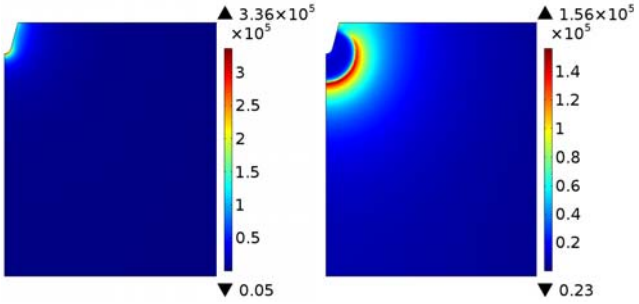

(a) *t*=0.18 ms (b) *t*=0.38 ms

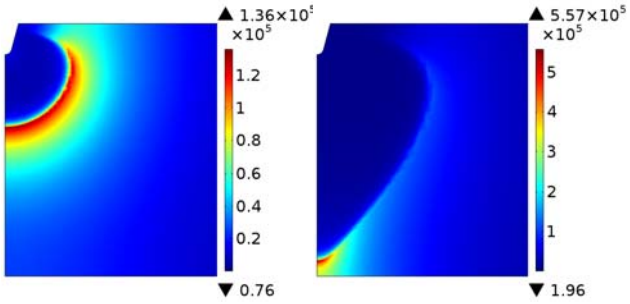

(c) *t*=0.58 ms (d) *t*=0.78 ms

Fig.6. Electric field distributions before the breakdown of needle-plate gap.

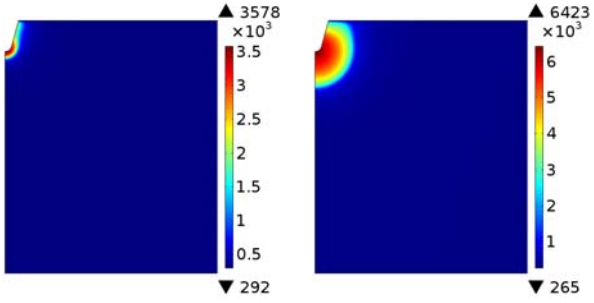

(a) *t*=0.18 ms (b) *t*=0.38 ms

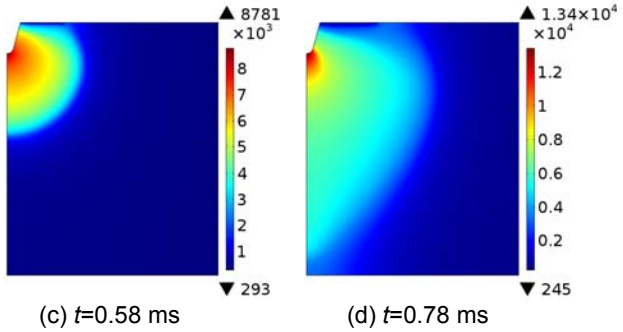

(c) *t*=0.58 ms (d) *t*=0.78 ms

Fig.7. Temperature field distributions before the breakdown of needle-plate gap.

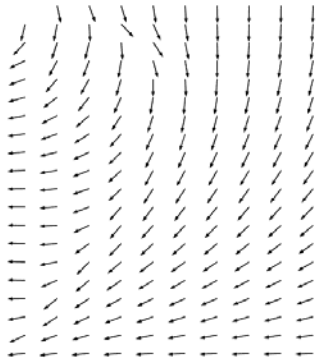

Fig.8. Lorentz force on the discharge arc.

It can be found that the discharge arc develops from the needle to the plate and the temperature of the discharge arc increases with time. The coupling relationship of these fields also can be found. The shape of the arc in the discharge process is caused by the Lorentz force, as shown in Fig.8.

In order to investigate the development velocity of the discharge arc, the temperature distribution curves along axis with four different times are given in Fig.9. It can be concluded that the development velocity of the discharge arc increases with the time. For example, when the time is from 0.18 ms to 0.38 ms, the discharge arc develops 1.3 mm; when the time is from 0.58 ms to 0.78 ms, the discharge arc develops 5.6 mm.

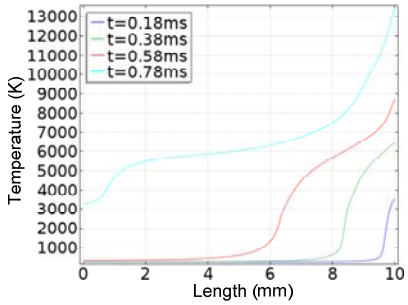

Fig.9. Temperature distribution curves along axis with different time.

Conclusion

A needle-plate discharge model in atmospheric air based on MHD theory is built. Based on this method, the distributions of the electric potential, electric field, temperature field in the discharge process are investigated, and the coupling relationship is validated.

From simulation results and analysis, some conclusions can be drawn as follows:

1) Once the needle-plate gap is a breakdown, the voltage is instantly decreased and the discharge current is instantly increased.

2) Due to the Lorentz force, the arc radius decreases in the discharge process.

3) The development velocity of the discharge arc increases with the time before breakdown.

ACKNOWLEDGMENT

This work was supported by the East Inner Mongolia Electric Power Company Limited, the National Natural Science Foundation of China (Grant No. 51477013), the Major State Basic Research Development Program of China (973 Program, No. 2011CB209401) and the Fundamental Research Funds for Central Universities (No. CDJZR14155501).

Authors: Cheng Peng, Yang Fan and Yang Qi are with the State Key Laboratory of Power Transmission Equipment & System Security and New Technology, School of Electrical Engineering, Chongqing University, Chongqing 400044 China (e-mail: chengpeng19870825@163.com).

Luo Hanwu, Liu Haibo and Kang Kai are with East Inner Mongolia Electric Power Company Limited, Hohhot 010020, China.

REFERENCES

[1] M. Iwata, et al, CFD calculation of pressure rise due to internal AC and DC arcing in a closed container, IEEE Trans. Power. Del., vol. 26, no. 3, pp. 1700-1709, Jul. 2011.

[2] B H Bang, et al, Prediction and improvement of dielectric breakdown between arc contacts in gas circuit breaker, 2nd International Conference on Electric Power Equipment, Matsue, Japan, 2013.

[3] Wu Yi, Rong Mingzhe, Wang Xiaohua, et al, Dynamic analysis of low-voltage air arc plasma during the contact opening process, Transactions of China Electrotechnical Society, vol. 23, no. 5, pp. 12-17, May, 2008.

[4] Yos J, Revised transport properties for high temperature air and its component, Avco Space Systems Division, Technical Release, 1967.

[5] Swierczynski B, Gonzalez J J, Teulet P, et al, Advances in low-voltage circuit breaker modeling, J.phys.D: Appl.Phy, vol. 37, no. 4, pp. 595-609, 2004.

[6] Gonzalez J J, Gleizes A, Mathematical modeling of a free-burning arc in the presence of metal vapor, J.Appl.Phys., vol. 74, no. 5, pp. 3065-3070, 1993.

[7] Lowke J J, Kovitya P, Schmidt H P, Theory of free-burning arc columns including the influence of the cathode, J. Phys. D: Appl. Phys., vol. 25, no. 6, pp. 1600-1606, 1992.

[8] Yang Yong, Wang Qiping, Computer aided numerical analysis of arcing processes in SF_6 circuit breaker nozzle, Proceedings of the CSEE, vol. 20, no. 5, pp. 9-13, 2000.

[9] M. Z. Rong, F. Yang, Y. Wu, A. B. Murphy, W. Z. Wang, and J. Guo, Simulation of arc characteristics in miniature circuit breaker, IEEE Trans. Plasma Sci., vol. 38, no. 9, pp. 2306-2310, Sep. 2010.

[10] Y. Wu, M. Z. Rong, X. W. Li, A. B. Murphy, X. H. Wang, F. Yang, and Z. Q. Sun, Numerical analysis of the effect of the chamber width and outlet area on the motion of an air arc plasma, IEEE Trans. Plasma Sci., vol. 36, no. 5, pp. 2831-2838, Oct. 2008.